Organosulphur–Transition-metal Chemistry. Part 7.[1] Sulphur Inversion in Dimolybdenum Complexes: Crystal and Molecular Structure of $[Mo_2(CO)_2\{P(OMe)_3\}(\mu\text{-}SBu^t)_3(\eta\text{-}C_7H_7)]$ †

By **Ian B. Benson, Selby A. R. Knox, Pamela J. Naish, and Alan J. Welch**, Department of Inorganic Chemistry, The University, Bristol BS8 1TS

Thiolato-bridged dimolybdenum complexes $[Mo_2(CO)_3(\mu\text{-}SR)_3(\eta\text{-}C_7H_7)]$ are formed by treating $[MoI(CO)_2(\eta\text{-}C_7H_7)]$ with RSH (R = Me, Et, Pr^i, or Bu^t) in the presence of NEt_3. Infrared and variable-temperature n.m.r. spectroscopy reveal that the complexes exist as two isomers, arising from different relative orientations of the R groups on bridging sulphur. At ambient temperatures and above, these isomers interconvert rapidly, attributed to a low-energy sulphur inversion process, such that complete averaging of R group environments is achieved on the n.m.r. time scale. Interconverting isomers are also present for the monosubstituted derivatives $[Mo_2(CO)_2(PR'_3)(\mu\text{-}SBu^t)_3(\eta\text{-}C_7H_7)]$ [R'_3 = $P(OMe)_3$, $PMePh_2$, PMe_2Ph, or PMe_3], but for these only a limited averaging is observed, generating a time-averaged mirror plane of molecular symmetry. This results from the presence of a phosphorus ligand *trans* to one bridging sulphur and of CO *trans* to the other two, shown in an *X*-ray diffraction study of $[Mo_2(CO)_2\{P(OMe)_3\}(\mu\text{-}SBu^t)_3(\eta\text{-}C_7H_7)]$. Crystals are monoclinic, space group $P2_1/n$, with four molecules in a unit cell of dimensions a = 10.186(7), b = 15.677(7), c = 19.821(15) Å, and β = 96.31(5)°. The structure has been solved by conventional techniques and refined by least squares to R 0.046 for 5 149 diffractometer-measured reflection intensities. Three bridging SBu^t groups display an asymmetric stereochemistry about a Mo–Mo bond [2.9460(15) Å], rationalised on the basis of intramolecular terminal ligand–bridging ligand contacts. One molybdenum is η^7 co-ordinated to a cycloheptatrienyl ring while the other carries the two CO groups and a $P(OMe)_3$ ligand. Metal–sulphur distances range over 2.411(2)—2.549(2) Å and Mo–P is 2.445(2) Å. Free energies of activation for sulphur inversion as low as 46 kJ mol^{-1} have been derived from coalescence temperatures for several complexes.

THE complexes $[\{Ru(CO)(\mu\text{-}SR)(\eta\text{-}C_5H_5)\}_2]$, described in Part 4 [2] of this series, exist as a variety of isomers. These arise from different relative orientations of the cyclopentadienyl ligands (*cis* and *trans*) and of the R groups on bridging sulphur (*syn* and *anti*). Only for *trans*-$[\{Ru(CO)(\mu\text{-}SCH_2Ph)(\eta\text{-}C_5H_5)\}_2]$ were *syn* and *anti* isomers observed to co-exist and these were shown to interconvert rapidly on the n.m.r. time scale *via* a sulphur inversion. As an extension of these studies, an attempt was made to prepare complexes $[\{Mo(CO)(\mu\text{-}SR)(\eta\text{-}C_7H_7)\}_2]$ (R = alkyl), analogous structurally to $[\{Ru(CO)(\mu\text{-}SR)(\eta\text{-}C_5H_5)\}_2]$. Previously Mohr *et al.*[3] had reported the synthesis of S-aryl molybdenum complexes of this formulation, by treating $[MoBr(CO)_2(\eta\text{-}C_7H_7)]$ with arenethiols and triethylamine. Their insolubility precluded adequate structural characterisation by i.r. and n.m.r. spectroscopy. We describe here the quite different products obtained when alkanethiols are employed, namely the complexes $[Mo_2(CO)_3(\mu\text{-}SR)_3(\eta\text{-}C_7H_7)]$ (1). This same observation was made contemporaneously by Mohr *et al.*,[4] but without they stud of isomerism and sulphur inversion reported below. A preliminary account of our work has appeared.[5]

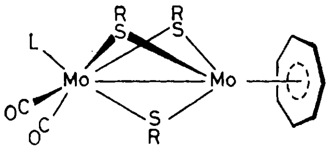

(1a; L = CO, R = Me)
(1b; L = CO, R = Et)
(1c; L = CO, R = Pr^i)
(1d; L = CO, R = Bu^t)
[1e; L = $P(OMe)_3$, R = Bu^t]
(1f; L = $PMePh_2$, R = Bu^t)
(1g; L = PMe_2Ph, R = Bu^t)
(1h; L = PMe_3, R = Bu^t)

RESULTS AND DISCUSSION

Complexes $[Mo_2(CO)_3(\mu\text{-}SR)_3(\eta\text{-}C_7H_7)]$.—Reactions at room temperature between $[MoI(CO)_2(\eta\text{-}C_7H_7)]$ and thiols RSH (R = Me, Et, Pr^i, or Bu^t) in the presence of triethylamine as an HI scavenger proceed in an extraordinary manner to provide a series of complexes $[Mo_2(CO)_3(\mu\text{-}SR)_3(\eta\text{-}C_7H_7)]$ (1a)—(1d), identified by i.r. and n.m.r. spectra (Table 1), mass spectra, and elemental analyses (Table 2). *X*-Ray diffraction studies have been performed on (1d)[4] and on trimethyl phosphite-substituted (1d), described below. Except for the reaction with Pr^iSH, (1a)—(1d) were the only sulphur–molybdenum complexes isolated, and were obtained in yields of 30—50%. With methanethiol, reaction was complete within 2 h, but for the remainder up to 2 d were required. Each of the dark red-black crystalline air- and solution-stable complexes displays a molecular ion in the mass spectrum, with characteristic Mo_2 isotope distribution, and six lower mass ions corresponding to loss of three carbonyls followed by three R groups from sulphur.

Infrared spectra of the complexes recorded in hexane solutions invariably show more than three and up to six carbonyl-stretching bands (Table 1). Some bands are broad, indicative of overlapping absorptions. Moreover, the relative intensities of the bands vary with the nature of the alkyl group. Clearly, these features must be due to the presence at room temperature of more than one isomer

---

† *f,g*-Dicarbonyl-*a*-η-cycloheptatrienyl-tri-μ-t-butylthio-*e*-(trimethyl phosphite)dimolybdenum(*Mo–Mo*).

TABLE 1

Infrared and ^1H n.m.r. data for the complexes

Complex	Carbonyl stretching bands (cm^{-1}) [a]	^1H n.m.r. spectrum (τ) [b]	
		Low-temperature limit	High-temperature limit
(1a) $[Mo_2(CO)_3(\mu\text{-}SMe)_3(\eta\text{-}C_7H_7)]$	2 002, 1 994 (sh), 1 954m, 1 882m, 1 867m	4.78 (s), 4.84 (s), 7.26 (s), 7.38 (s), 7.84 (s), 8.68 (s)	[c] 5.30 (s, 7 H), 8.02 (s, 9 H)
(1b) $[Mo_2(CO)_3(\mu\text{-}SEt)_3(\eta\text{-}C_7H_7)]$	2 001s, 1 958m, 1 950 (sh), 1 879w, 1 861s	4.74 (s), 4.79 (s), 6.84 (m), 7.64 (m), 8.21 (m), 8.30 (t, *J* 7), 8.35 (t, *J* 7), 9.14 (t, *J* 7)	[c] 5.15 (s, 7 H), 7.64 (q, *J* 7, 6 H), 8.75 (t, *J* 7, 9 H)
(1c) $[Mo_2(CO)_3(\mu\text{-}SPr^i)_3(\eta\text{-}C_7H_7)]$	2 000s, 1 953m, 1 944 (sh), 1 881w, 1 857s	4.69 (s), 4.70 (s), 6.99 (m), 7.25 (m), 7.97 (m), 8.29 (d, *J* 6), 8.32 (d, *J* 6), 8.54 (d, *J* 6), 8.55 (d, *J* 6), 8.58 (d, *J* 6), 8.84 (d, *J* 6), 8.92 (d, *J* 6), 9.19 (d, *J* 6)	[c] 4.70 (s, 7 H), 6.99 (spt, *J* 7, 3 H), 8.47 (d, *J* 7, 18 H)
(1d) $[Mo_2(CO)_3(\mu\text{-}SBu^t)_3(\eta\text{-}C_7H_7)]$	1 998s, 1 983m, 1 954m, 1 944 (sh), 1 882w, 1 851s	4.60 (s, 7 H), 8.48 (s, 9 H), 8.51 (s, 9 H), 9.01 (s, 9 H)	4.66 (s, 7 H), 8.67 (s, 27 H)
(1e) $[Mo_2(CO)_2\{P(OMe)_3\}(\mu\text{-}SBu^t)_3(\eta\text{-}C_7H_7)]$	1 956s, br, 1 816s, br	4.76 (s, 7 H), 6.44 (d, *J* 11, 9 H), 8.58 (s, 9 H), 8.66 (s, 9 H), 9.11 (s, 9 H)	4.73 (s, 7 H), 6.37 (d, *J* 11, 9 H), 8.47 (s, 9 H), 8.77 (s, 18 H)
(1f) $[Mo_2(CO)_2(PMePh_2)(\mu\text{-}SBu^t)_3(\eta\text{-}C_7H_7)]$	1 936m, 1 923m, 1 807s, br	2.51 (m, 10 H), 4.64 (s, 7 H), 7.70 (s, br, 3 H), 8.45 (s, 9 H), 8.95 (s, 9 H), 9.14 (s, 9 H)	2.52 (m, 10 H), 4.66 (s, 7 H), 7.70 (d, *J* 8, 3 H), 8.40 (s, 9 H), 8.96 (s, 18 H)
(1g) $[Mo_2(CO)_2(PMe_2Ph)(\mu\text{-}SBu^t)_3(\eta\text{-}C_7H_7)]$	1 935s, 1 925s, 1 812 (sh), 1 808s	2.58 (m, 5 H), 4.64 (s, 7 H), 8.10 (s, br, 6 H), 8.43 (s, 9 H), 8.79 (s, 9 H), 8.97 (s, 9 H)	2.58 (m, 5 H), 4.68 (s, 7 H), 8.10 (d, *J* 8, 6 H), 8.43 (s, 9 H), 8.86 (s, 18 H)
(1h) $[Mo_2(CO)_2(PMe_3)(\mu\text{-}SBu^t)_3(\eta\text{-}C_7H_7)]$	1 934s, br, 1 808s, br	4.68 (s, 7 H), 8.40 (d, *J* 7, 9 H), 8.50 (s, 9 H), 8.54 (s, 9 H), 9.01 (s, 9 H)	4.66 (s, 7 H), 8.33 (d, *J* 7 9 H), 8.41 (s, 9 H), 8.68 (s, 18 H)

[a] In hexane. [b] Relative intensities are given in parentheses; *J* in Hz. In $CDCl_3$, unless otherwise stated. [c] In PhCl.

of each complex. If the relative orientations of the R groups and lone pairs on bridging sulphur are considered it can be seen that two isomers are indeed possible; the symmetric and asymmetric arrangements (S) and (A), viewed along the Mo–Mo axis.

TABLE 2

Physical, analytical, and mass-spectral data for the complexes

Complex	M.p. (θ_c/°C) [a]	Colour	Analysis (%) [b]			
			C	H	S	*M* [b]
(1a)	82	Black	30.5	3.1	18.9	508
			(30.7)	(3.2)	(18.9)	(508)
(1b)	88	Black	34.6	4.0	17.0	550
			(34.9)	(4.0)	(17.4)	(550)
(1c)	100	Black	38.2	4.7	16.0	592
			(38.5)	(4.7)	(16.2)	(592)
(1d)	115	Black	42.0	5.7	15.3	634
			(41.6)	(5.4)	(15.1)	(634)
(1e)	158	Black	39.6	6.3	13.3	730
			(39.5)	(5.9)	(13.2)	(730)
(1f)	147	Black	50.6	5.8	11.9	200 [c]
			(50.8)	(6.3)	(11.7)	(806)
(1g)	153	Black	47.1	6.3	12.9	138 [c]
			(46.8)	(6.1)	(12.9)	(744)
(1h)	152	Dark brown	41.6	6.4	13.6	682
			(42.2)	(6.3)	(14.1)	(682)

[a] With decomposition. [b] Calculated values are given in parentheses. [c] Heaviest ion observed ($PR'_3{}^+$).

N.m.r. spectra of the complexes (1a)—(1d) confirmed the existence of the two isomers and revealed that these interconvert rapidly at or above room temperature. The ^1H n.m.r. spectrum of (1a) in the SMe region between −60 and 120 °C is presented in Figure 1. At −60 °C there are three methyl group signals of equal intensity at τ 7.26, 7.38, and 8.68 which correspond to isomer (A) and one at τ 7.84 corresponding to the equivalent methyl groups of isomer (S). From their relative intensities the ratio of (S) : (A) at this temperature is 1 : 3. This is confirmed by the observation of two singlets at τ 4.78 and 4.84 with the same relative intensities, due to the η-C_7H_7 ligand of each isomer. On warming, broadening then coalescence of signals occurs until at 120 °C the spectrum comprises singlets at τ 5.30 (7 H, C_7H_7) and 8.02 (9 H, $3SCH_3$). These changes, which are reversed on cooling, are attributed to the onset of rapid pyramidal inversion of the bridging sulphur atoms. This effects an (S) $\rightleftharpoons$ (A) interconversion and consequent averaging of environments of both the C_7H_7 and SMe group protons on the n.m.r. time scale.

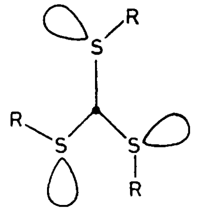

(S)

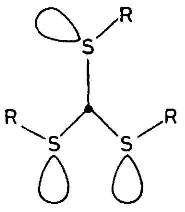

(A)

Similar behaviour is observed for (1b) and (1c), whose ^1H n.m.r. spectra as a function of temperature are displayed in Figures 2 and 3 respectively. These spectra are complicated by the prochiral character of the sulphur atoms. For (1b) this is reflected in anisochronous methylene protons, which appear at low temperatures as

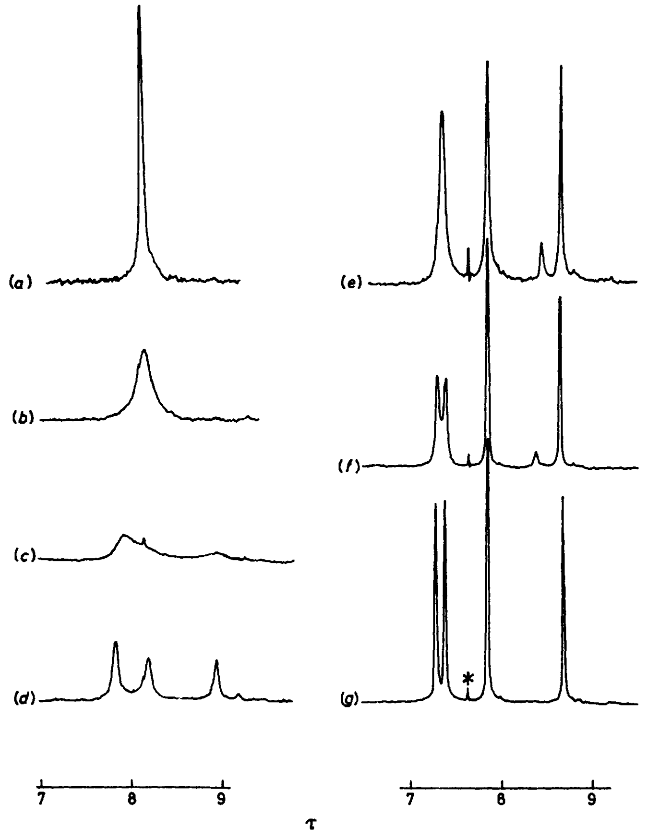

FIGURE 1 Proton n.m.r. spectrum of (1a) at various temperatures in PhCl: 120 (*a*); 90 (*b*); 50 (*c*); 30 (*d*); 20 (*e*); 0 (*f*); and −60 °C (*g*). Impurity denoted by asterisk

an array of overlapping quartets in the range τ 6—8. The consequence for (1c) is that the methyls of each isopropyl group are anisochronous.

The limiting low-temperature spectrum of the ethyl complex (1b) clearly indicates the dominant presence of asymmetric isomer (A), shown by the three triplets of equal intensity centred at τ 8.30, 8.35, and 9.14, and at lower concentration of isomer (S), whose equivalent ethyl groups have a single methyl signal at τ 8.67. The relative intensities of these signals correspond to an (S) : (A) ratio of 1 : 6, as do those of the two C_7H_7 signals at τ 4.74 and 4.79. The limiting (−20 °C) spectrum of the isopropyl analogue (1c) is not interpreted so readily. Two C_7H_7 signals are observed, but so close in shift as to make calculation of an (S) : (A) ratio unreliable. It appears, however, that the proportion of the symmetric isomer has declined still further with increase in size of the alkyl group. Although the two isomers of (1c) provide a total of four Pr^i group environments at −20 °C the methyl groups within each are inequivalent, as described above, and eight doublets are seen. Assignment of these to a particular isomer was not achieved. On warming both (1b) and (1c) to 120 °C, spectra are obtained which are consistent with the generation of time-averaged equivalence of alkyl group environments. Both the methylene protons of (1b) and the methyl groups of (1c) are now isochronous; *i.e.* the prochirality of the sulphur atoms has been lost. This would be a direct result of a sulphur-inversion process for (S) $\rightleftharpoons$ (A) interconversion.

The ^1H n.m.r. spectra (Figure 4) obtained for the t-butyl complex (1d) are considerably more simple than those of the other complexes in this series. The trend towards an increased proportion of isomer (A) with increasing size of alkyl group reaches its limit and at −45 °C only this isomer can be detected by n.m.r. spectroscopy, showing signals for the three Bu^t groups at τ 8.48, 8.51, and 9.01 and for a single η-C_7H_7 environment at τ 4.60. This correlates with the solid-state structure of (1d), which was found to adopt the (A) configuration.[4] Again, inversion is initiated on warming

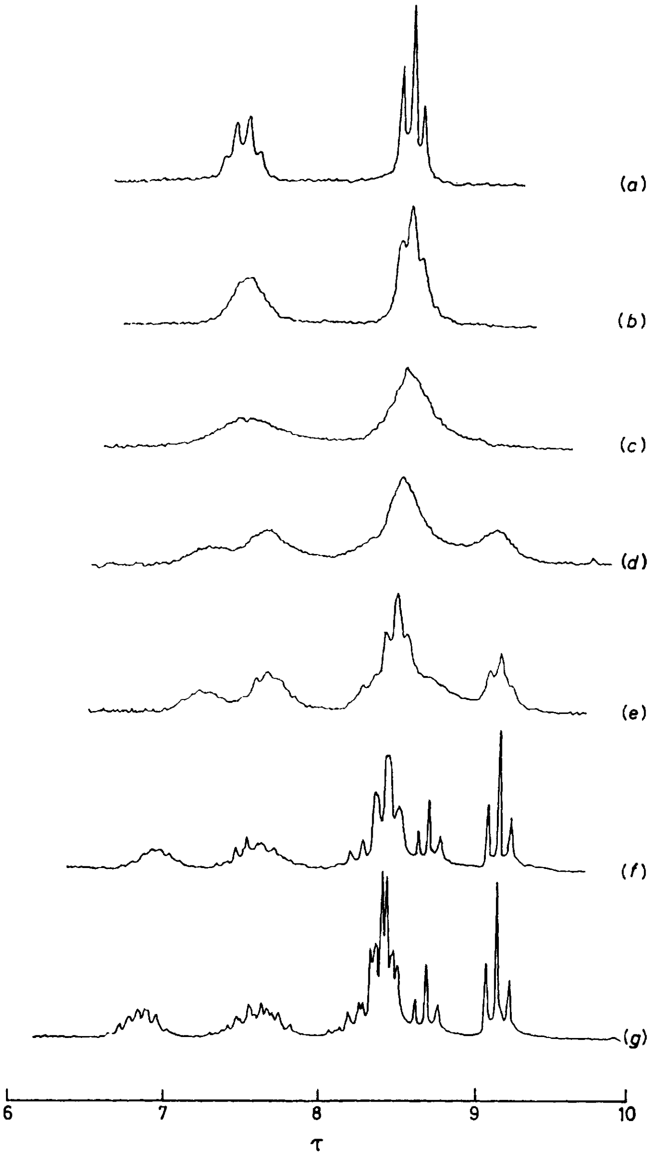

FIGURE 2 Proton n.m.r. spectrum of (1b) at various temperatures in PhCl: 120 (*a*); 100 (*b*); 80 (*c*); 50 (*d*); 30 (*e*); 0 (*f*); and −60 °C (*g*)

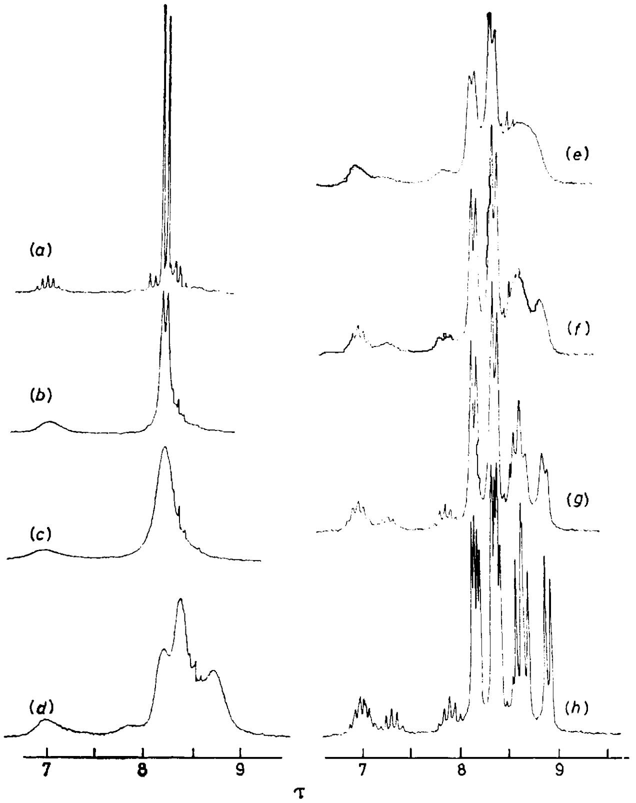

FIGURE 3 Proton n.m.r. spectrum of (1c) at various temperatures in PhCl: 120 (*a*); 80 (*b*); 60 (*c*); 40 (*d*); 30 (*e*); 20 (*f*); 0 (*g*); and −20 °C (*h*)

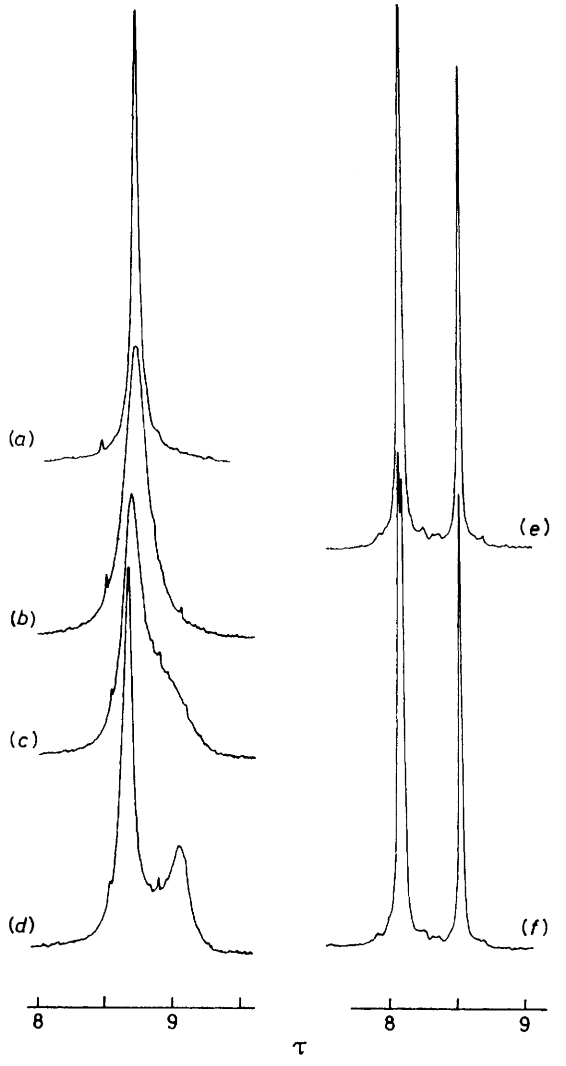

FIGURE 4 Proton n.m.r. spectrum of (1d) at various temperatures in $CDCl_3$: 30 (*a*); 10 (*b*); 1 (*c*); −4 (*d*); −33 (*e*); and −45 °C (*f*)

and the Bu^t group signals coalesce to a sharp singlet (τ 8.67) at 30 °C as a result of rapid (A) $\rightleftharpoons$ (S) interconversion.

Complexes $[Mo_2(CO)_2(PR_3')(\mu\text{-}SR)_3(\eta\text{-}C_7H_7)]$.—Reactions of $[Mo_2(CO)_3(\mu\text{-}SBu^t)_3(\eta\text{-}C_7H_7)]$ (1d) with phosphines were studied with a view to substituting one or more carbonyls, in order that the effects of these powerful σ donors on the inversion process could be determined. In boiling hexane, the Bu^t complex (1d) was found to react with $P(OMe)_3$, $PMePh_2$, PMe_2Ph, or PMe_3 to give the black, crystalline monosubstituted products $[Mo_2(CO)_2(PR'_3)(\mu\text{-}SBu^t)_3(\eta\text{-}C_7H_7)]$ (1e)—(1h). As with the unsubstituted precursors, evidence for the existence of isomers (S) and (A) in solution at room temperature was provided by i.r. spectroscopy, the PMe_2Ph complex showing four distinct carbonyl-stretching frequencies. The other three complexes displayed two broad asymmetric bands indicative of two pairs of overlapping absorptions. One of the more interesting (and unexpected) results of the variable-temperature n.m.r. studies on the complexes (1) is the observation that adoption of the asymmetric structure (A) is, at reduced temperature, favoured over the symmetric alternative (S) and, furthermore, that as the size of the alkyl group R is increased the isomeric separation becomes more acute. Such results are opposed to predictions based on the assumption that the minimisation of intramolecular bridge–bridge (R · · · R) contacts determines the overall stereochemistry, and an explanation of this was sought in an *X*-ray diffraction study of (1e).

In Figure 5 a single molecule is viewed in a direction perpendicular to the metal–metal vector. Interatomic distances (uncorrected for thermal effects) and selected interbond angles are presented in Tables 3 and 4 respectively. The analysis reveals that, in the solid state, the compound (1e) adopts the asymmetric configuration (A). This is more easily seen in Figure 6, which is a view along the Mo–Mo bond. It is apparent that not only do the three bridging SBu^t groups adopt the arrangement (A) as defined by the S–C vectors, but that the sulphur atoms themselves are unevenly disposed about the metal–metal link. If the centre of the Mo(1)–Mo(2) bond is defined by a point X, then S–X–S angles are found to decrease in the sequence S(1)–X–S(2) 159.3, S(2)–X–S(3) 107.9, and S(1)–X–S(3) 92.4°. An alternative description could employ non-bonded S · · · S distances,

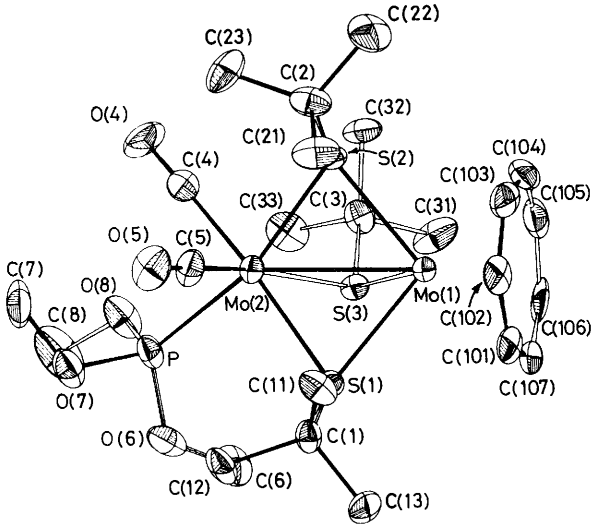

FIGURE 5 Perspective view of (1e), with atomic numbering scheme. Thermal ellipsoids are constructed at the 30% probability level

viz. S(1) · · · S(2) 3.890(3), S(2) · · · S(3) 3.256(3), and S(1) · · · S(3) 2.939(3) Å.

From Figure 6 it is clear that the direction of the S–C vectors at S(1) and S(3) are such that their Bu^t groups point away from the $P(OMe)_3$ ligand. Although hydrogen atoms were not located in the structural determination we have searched for close interligand (terminal–bridge) contacts, assuming an effective van der Waals radius for a methyl group of 2.0 Å. It arises that the distances O(6) · · · C(12) [3.496(10)] and O(8) · · · C(33) [3.564(10) Å] could both undoubtedly be reduced to well below the O · · · Me van der Waals sum (3.4 Å) were alternative conformations adopted at S(1) and S(3).

TABLE 3

Bond lengths (Å) for (1e) *

Mo(1)–Mo(2)	2.946 0(15)	S(1)–C(1)	1.885(7)
Mo(1)–S(1)	2.523(2)	C(1)–C(11)	1.533(9)
Mo(1)–S(2)	2.483(2)	C(1)–C(12)	1.538(9)
Mo(1)–S(3)	2.549(2)	C(1)–C(13)	1.548(9)
Mo(1)–C(101)	2.294(8)		
Mo(1)–C(102)	2.324(7)	S(2)–C(2)	1.874(7)
Mo(1)–C(103)	2.309(7)	C(2)–C(21)	1.535(11)
Mo(1)–C(104)	2.322(7)	C(2)–C(22)	1.569(12)
Mo(1)–C(105)	2.295(8)	C(2)–C(23)	1.547(11)
Mo(1)–C(106)	2.282(7)		
Mo(1)–C(107)	2.336(7)	S(3)–C(3)	1.881(7)
		C(3)–C(31)	1.537(11)
Mo(2)–S(1)	2.444(2)	C(3)–C(32)	1.518(10)
Mo(2)–S(2)	2.411(2)	C(3)–C(33)	1.522(10)
Mo(2)–S(3)	2.534(2)		
Mo(2)–P	2.445(2)	C(4)–O(4)	1.149(9)
Mo(2)–C(4)	2.009(7)	C(5)–O(5)	1.175(10)
Mo(2)–C(5)	1.931(8)		
		P–O(6)	1.594(6)
C(101)–C(102)	1.413(11)	P–O(7)	1.606(6)
C(102)–C(103)	1.389(11)	P–O(8)	1.596(6)
C(103)–C(104)	1.412(13)	O(6)–C(6)	1.465(11)
C(104)–C(105)	1.373(12)	O(7)–C(7)	1.445(12)
C(105)–C(106)	1.409(11)	O(8)–C(8)	1.469(10)
C(106)–C(107)	1.417(12)		
C(107)–C(101)	1.408(13)		

* Throughout the Tables of crystallographic data, estimated standard deviations are given in parentheses.

TABLE 4

Bond angles (°) for (1e)

Mo(2)–Mo(1)–S(1)	52.39(5)	Mo(1)–S(1)–Mo(2)	72.73(4)
Mo(2)–Mo(1)–S(2)	51.88(4)	Mo(1)–S(1)–C(1)	124.5(2)
Mo(2)–Mo(1)–S(3)	54.34(4)	Mo(2)–S(1)–C(1)	118.7(2)
S(1)–Mo(1)–S(2)	101.98(5)	S(1)–C(1)–C(11)	113.0(5)
S(1)–Mo(1)–S(3)	70.81(6)	S(1)–C(1)–C(12)	106.3(4)
S(2)–Mo(1)–S(3)	80.63(5)	S(1)–C(1)–C(13)	105.5(5)
C(101)–Mo(1)–C(102)	35.6(3)	C(11)–C(1)–C(12)	110.9(6)
C(102)–Mo(1)–C(103)	34.9(3)	C(11)–C(1)–C(13)	111.4(6)
C(103)–Mo(1)–C(104)	35.5(3)	C(12)–C(1)–C(13)	109.5(6)
C(104)–Mo(1)–C(105)	34.6(3)		
C(105)–Mo(1)–C(106)	35.9(3)	Mo(1)–S(2)–Mo(2)	74.01(5)
C(106)–Mo(1)–C(107)	35.7(3)	Mo(1)–S(2)–C(2)	122.8(2)
C(107)–Mo(1)–C(101)	35.4(3)	Mo(2)–S(2)–C(2)	118.3(3)
		S(2)–C(2)–C(21)	113.4(5)
Mo(1)–Mo(2)–S(1)	54.88(4)	S(2)–C(2)–C(22)	105.3(5)
Mo(1)–Mo(2)–S(2)	54.11(5)	S(2)–C(2)–C(23)	105.5(5)
Mo(1)–Mo(2)–S(3)	54.83(5)	C(21)–C(2)–C(22)	113.0(6)
Mo(1)–Mo(2)–P	138.70(6)	C(21)–C(2)–C(23)	109.8(7)
Mo(1)–Mo(2)–C(4)	128.7(2)	C(22)–C(2)–C(23)	109.5(6)
Mo(1)–Mo(2)–C(5)	114.9(2)		
S(1)–Mo(2)–S(2)	106.50(5)	Mo(1)–S(3)–Mo(2)	70.83(6)
S(1)–Mo(2)–S(3)	72.35(6)	Mo(1)–S(3)–C(3)	123.9(2)
S(1)–Mo(2)–P	90.92(6)	Mo(2)–S(3)–C(3)	119.6(2)
S(1)–Mo(2)–C(4)	168.0(2)	S(3)–C(3)–C(31)	106.6(5)
S(1)–Mo(2)–C(5)	95.9(2)	S(3)–C(3)–C(32)	113.5(5)
S(2)–Mo(2)–S(3)	82.32(6)	S(3)–C(3)–C(33)	105.7(5)
S(2)–Mo(2)–P	160.97(6)	C(31)–C(3)–C(32)	110.5(6)
S(2)–Mo(2)–C(4)	81.2(2)	C(31)–C(3)–C(33)	110.3(6)
S(2)–Mo(2)–C(5)	97.2(2)	C(32)–C(3)–C(33)	110.0(6)
S(3)–Mo(2)–P	96.13(7)		
S(3)–Mo(2)–C(4)	100.1(2)	Mo(2)–C(4)–O(4)	179.5(6)
S(3)–Mo(2)–C(5)	167.4(2)	Mo(2)–C(5)–O(5)	179.1(6)
P–Mo(2)–C(4)	80.4(2)		
P–Mo(2)–C(5)	88.3(2)	Mo(2)–P–O(6)	121.5(2)
C(4)–Mo(2)–C(5)	92.2(3)	Mo(2)–P–O(7)	120.9(2)
		Mo(2)–P–O(8)	110.8(2)
C(107)–C(101)–C(102)	130.4(7)	O(6)–P–O(7)	92.7(3)
C(101)–C(102)–C(103)	125.8(7)	O(6)–P–O(8)	105.7(3)
C(102)–C(103)–C(104)	130.2(7)	O(7)–P–O(8)	102.4(3)
C(103)–C(104)–C(105)	129.3(7)	P–O(6)–C(6)	120.9(5)
C(104)–C(105)–C(106)	128.2(8)	P–O(7)–C(7)	120.3(5)
C(105)–C(106)–C(107)	128.3(8)	P–O(8)–C(8)	121.7(5)
C(106)–C(107)–C(101)	127.5(7)		

The observed directions of the S(1)–C(1) and S(3)–C(3) vectors demand an overall type (A) stereochemistry. Given that, in the crystal, the S(2)–C(2) vector leans

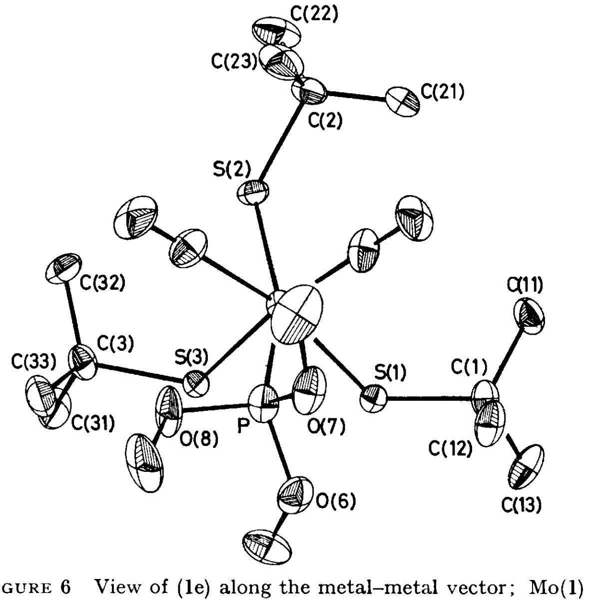

FIGURE 6 View of (1e) along the metal–metal vector; Mo(1) and the C_7H_7 ring are omitted for clarity

towards the C(1)Me_3 unit, the disposition of methyl groups at C(2) and the greater S(1) · · · S(2) distance over S(2) · · · S(3) are totally compatible with C(32) bisecting the C(22)–C(2)–C(23) angle and thus requiring that C(21) and C(11) approach to within 4.020(10) Å. It would be expected that inversion at S(2) be energetically more accessible than inversion at S(1) or S(3) on the basis of the above results.

It is worthwhile to emphasise that, even with bulky Bu^t groups, a type (A) stereochemistry need not necessarily involve highly unfavourable R · · · R interbridge contacts since the three sulphur atoms are apparently not rigidly held at S–X–S angles of 120°. Thus C(11) · · · C(21) is only on the *verge* of the van der Waals sum. Furthermore, the relative orientation of the S(2) Bu^t and S(3) Bu^t groups is that found in the symmetric form (S) and, as such, represents a useful model. Although the Bu^t groups adopt a relative geometry which minimises steric congestion, neither of the nearest-neighbour interactions C(32) · · · C(22) and C(32) · · · C(23) are important at 5.168(12) and 5.351(11) Å respectively. Perhaps more relevant is the S(2)–X–S(3) angle which, at 107.9°, is well below the value of 120° required by a symmetric (locally C_{3h}) isomer.

Thus, for the phosphite-substituted complex (1e) it is almost certainly intramolecular contacts between the terminal phosphite and bridging SBu^t ligands which are most important in favouring molecules with a type (A) stereochemistry. For the unsubstituted species (1d) the preference for stereoisomer (A) over (S) would be expected to be less pronounced. Nevertheless, the asymmetric form (A) is still favoured (even for methyl) and it therefore seems probable that a terminal–bridge interligand interaction of the type described above may still be significant. Since such a conclusion is rather unexpected we have examined the molecular structure [4] of (1d) (A form) for OC · · · Bu^t contacts. Unfortunately, the van der Waals radius for a carbon atom in the carbonyl environment is not well documented, but it is unlikely to be less than that of a nitrogen atom (1.5 Å). For (1e) there are five OC · · · Me distances between 3.4 and 3.5 Å (Table 5) and, of course, the S–X–S angles which the carbonyls bisect here are the widest. It therefore seems that contacts of this type may indeed be important in (1a)—(1d).

The Mo(1)–Mo(2) distance for (1e) is 2.9460(15) Å and the metal–metal vector may be taken to lie in the capping direction of a distorted capped-octahedral geometry at each metal centre. Mo–Mo separations in comparable (Mo^{II}) compounds are 2.933(1) Å in $[Mo_2(CO)_3(\mu\text{-}SBu^t)_3(\eta\text{-}C_7H_7)]$ (1d),[4] 2.882(2) Å in $[Mo_2(\mu\text{-}Br)(\mu\text{-}OH)_2(\eta\text{-}C_7H_7)_2]^+$,[6] and an average of 3.068 Å found in independent structural determinations of $[Mo_2(\mu\text{-}Cl)_3(\eta\text{-}C_7H_7)_2]^+$.[7,8] The molecule $[Mo_2(CO)_4(\mu\text{-}Br)_2(\eta\text{-}C_4Ph_4)_2]$ is also a molybdenum(II) species if the metal–metal bond, 2.954(1) Å, is included.[9]

Molybdenum–sulphur distances fall within the range 2.411(2)—2.549(2) Å, which in general represents an extension of the values typically found [10–13] for sulphur atoms bridging two molybdenums in formal oxidation states of +V and +IV, and all three sulphur atoms are individually found to favour Mo(2) in forming slightly asymmetric Mo–S bonds. Furthermore, in spite of the existence of the terminal · · · bridge contacts across Mo(2) that we have already discussed, the Bu^t groups on each sulphur bend slightly towards Mo(2). This is clearly evident from a comparison of Mo(1)–S–C and Mo(2)–S–C angles, 122.8—124.5 and 118.3—119.6° respectively. Finally, we note that Mo(1)–C(cycloheptatrienyl) distances, 2.282—2.336 Å, are rather longer than might be expected.[6] All three features might be rationalised by non-bonding interactions * between the cycloheptatrienyl ring and the bridging Bu^t functions and, indeed, several contacts exist (Table 5) between ring-carbon atoms and methyl groups that are within the van der Waals sum assuming a half-thickness of 1.85 Å for the aromatic ring.

TABLE 5

Relevant non-bonding distances (Å) for (1e)

(*a*) Phosphite · · · Bu^tS			
O(6) · · · C(12)	3.496(10)	O(8) · · · C(33)	3.564(10)
(*b*) Carbonyl · · · Bu^tS			
C(4) · · · C(23)	3.496(11)	C(5) · · · C(21)	3.402(11)
C(5) · · · C(12)	3.457(11)	C(5) · · · C(23)	3.474(11)
C(5) · · · C(11)	3.479(10)		
(*c*) SBu^t · · · Bu^tS			
C(11) · · · C(21)	4.020(10)	C(32) · · · C(23)	5.351(11)
C(32) · · · C(22)	5.168(12)		
(*d*) Cycloheptatrienyl · · · Bu^tS			
C(101) · · · C(11)	3.738(11)	C(102) · · · C(21)	3.831(12)
C(101) · · · C(13)	3.748(11)	C(103) · · · C(21)	3.606(12)
C(102) · · · C(11)	3.742(11)	C(103) · · · C(22)	3.667(12)
(*e*) Intermolecular *			
C(104) · · · C(12^{I})	3.266(10)	C(11) · · · C(8^{III})	3.383(11)
C(31) · · · C(13^{II})	3.553(11)		

* Roman numeral superscripts define the following equivalent positions relative to the reference molecule at x, y, z: I $1 + x, y, z$; II $-x, -y, -z$; III $\frac{1}{2} + x, \frac{1}{2} - y, \frac{1}{2} + z$. Contacts (*a*)—(*d*) are all intramolecular.

The carbon atoms of the cycloheptatrienyl ring define a regular heptagon and a plane whose equation is $-7.804x + 9.053y - 3.855z = -0.987$ Å, where x, y, and z are the atomic co-ordinates (direct space, Table 6). The standard deviation of the seven atoms from this plane is less than 0.03 Å. The atom Mo(1) is 1.649 Å from the ring plane and, in projection, is displaced only slightly (<0.016 Å) from its centre. However, the normal to the ring is not collinear with the metal–metal vector, deviating (by *ca.* 4.5°) roughly towards S(3). This feature is clearly visible in Figure 5, and we take it to be a direct consequence of the fact that the Mo(1)–S(3) distance is the longest of its type, the three *fac*

---

* A recent attempt [14] to evaluate the relative bonding capabilities of $M(CO)_3$ and M(polyene) fragments with a main-group probe (which might have provided an electronic explanation of the uneven bridge distances) was unfortunately inconclusive.

TABLE 6

Atomic positional parameters as fractional co-ordinates ($\times 10^5$ for Mo, S, P; $\times 10^4$ for C, O) for (1e)

Atom	x	y	z
Mo(1)	6 220(5)	16 824(3)	9 680(3)
Mo(2)	−16 894(5)	28 015(3)	6 591(2)
S(1)	−17 850(14)	12 838(9)	9 310(7)
C(1)	−2 617(6)	948(4)	1 692(3)
C(11)	−1 948(8)	1 313(5)	2 361(3)
C(12)	−4 058(7)	1 253(5)	1 559(4)
C(13)	−2 580(8)	−39(4)	1 693(2)
S(2)	5 317(16)	32 629(9)	10 283(8)
C(2)	835(8)	3 865(5)	1 847(3)
C(21)	412(9)	3 375(5)	2 459(4)
C(22)	2 345(9)	4 089(6)	1 925(5)
C(23)	17(10)	4 695(5)	1 738(4)
S(3)	−5 344(15)	19 939(9)	−2 130(7)
C(3)	246(7)	2 600(4)	−884(3)
C(31)	1 029(10)	1 947(5)	−1 258(4)
C(32)	1 140(8)	3 320(4)	−602(4)
C(33)	−895(9)	2 957(6)	−1 361(4)
P	−38 977(16)	27 401(13)	372(9)
O(6)	−4 613(5)	1 853(4)	−147(3)
O(7)	−5 155(5)	3 116(4)	361(3)
O(8)	−3 942(5)	3 250(4)	−662(3)
C(6)	−3 989(9)	1 204(6)	−537(5)
C(7)	−5 175(10)	3 997(6)	572(6)
C(8)	−5 167(9)	3 333(8)	−1 122(5)
C(4)	−1 772(7)	3 970(4)	241(4)
O(4)	−1 827(7)	4 637(3)	−1(3)
C(5)	−2 490(7)	3 195(4)	1 441(4)
O(5)	−2 987(6)	3 441(4)	1 912(3)
C(101)	993(7)	467(5)	1 605(5)
C(102)	1 573(7)	1 146(5)	2 001(4)
C(103)	2 420(7)	1 757(5)	1 785(4)
C(104)	2 896(7)	1 867(5)	1 148(5)
C(105)	2 602(7)	1 411(5)	558(4)
C(106)	1 796(8)	682(5)	452(4)
C(107)	1 126(8)	231(4)	930(5)

Mo(1) orbitals used to bind the ring being directionally * distorted in a small but nevertheless similar fashion to that previously observed [6] in the complex $[Mo_2(\mu\text{-}Br)(\mu\text{-}OH)_2(\eta\text{-}C_7H_7)_2]^+$.

Although we have not been able to locate the ring-hydrogen atoms there is now a clear precedent [15] for supposing them to be slightly out of the C_7 plane (at an elevation angle of the order of 10°) on the same side as the metal atom.

The spread of Mo–S distances is considerably greater at Mo(2) than at Mo(1) and this feature may be traced to the differing types of terminal ligand bound to the former metal. The shortest Mo(2)–S bond is *trans* to the phosphite group, which substantiates the better π-acceptor property of CO over $P(OMe)_3$. An Mo–P bond length of 2.445(2) Å is towards the upper limit of the range of similar values, 2.388—2.470 Å, sampled from the literature,[16-18] and is consistent with this ligand competing for metal *d*-orbital density with other fairly strong π acids.[17] As expected,[19] the Mo–P–O angles (110.8—121.5°) are consistently wider than the O–P–O type (92.7—105.7°), although we here refrain from comparing average angles (as has previously been the habit) since each internal spread is of the same order of magnitude as the difference between mean values.

The distances Mo(2)–C(4), **2.009(7)** Å, and Mo(2)–C(5), **1.931(8)** Å, are significantly different, as are (just) the C(4)–O(4) and C(5)–O(5) separations, 1.149(9) and 1.175(10) Å respectively. Differences between corresponding lengths in these Mo–C–O spines are entirely consistent with differing *trans* effects of the asymmetrically bonded sulphur atoms S(1) and S(3). It is unclear exactly why S(3) is so much further from the metal centres than the chemically equivalent S(1), although the asymmetry inherent in a type (A) stereoisomer *via* the intramolecular contacts previously discussed could, in this particular case, be compounded with intermolecular interactions. The three most severe of these are listed in Table 4, and each may be seen to involve a methyl group of at least one of each of the SBu^t fragments. The overall crystal packing is reproduced in Figure 7.

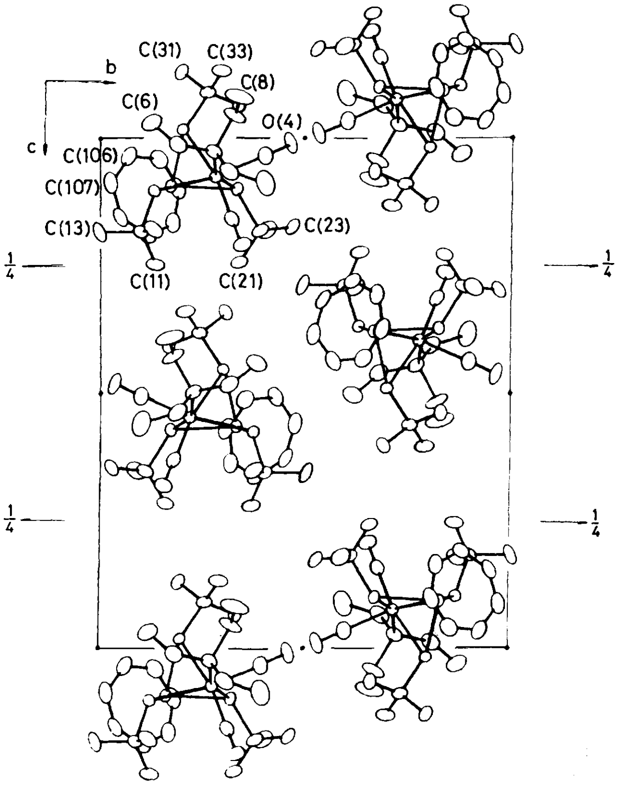

FIGURE 7 Contents of one unit cell of (1e), as seen along the $-a^*$ axis, looking towards the origin. Only the minimum number of symmetry elements to describe the array are shown for clarity

The observation that the $P(OMe)_3$ ligand in (1e), and by implication the phosphine ligand in (1f)—(1h), is *trans* to one of the μ-SBu^t groups while the two carbonyls are *trans* to the remaining two μ-SBu^t groups allows a ready interpretation of the variable-temperature n.m.r. behaviour of (1e)—(1h). In (1d), as in (1a)—(1c), complete averaging of R group environments is achieved on the n.m.r. time scale at high temperatures. However, for each of the PR_3-substituted derivatives (1e)—(1h) only limited averaging occurs. The spectrum of (1e) is

---

* Consistent with the direction of tilt is the observation that the shortest $C_7 \cdots Bu^t$ contacts involve the methyl groups bound to C(1) and C(2).

typical and is presented in Figure 8. At −53 °C signals are seen at τ 4.76 (s, C_7H_7), 6.44 [d, *J* 11 Hz, $P(OCH_3)_3$], 8.58 (s, C_4H_9), 8.66 (s, C_4H_9), and 9.11 (s, C_4H_9), characteristic of the presence of the (A) isomer alone. On warming, broadening and coalescence of the two high-field Bu^t group signals occurs so that at 62 °C the spectrum comprises resonances at τ 4.73 (s, C_7H_7), 6.37 [d, *J* 11 Hz, $P(OCH_3)_3$], 8.47 (s, C_4H_9), and 8.77 (s, $2C_4H_9$). Heating to 150 °C achieved no further coalescence. Clearly, a time-averaged mirror plane of molecular symmetry has been generated, and on the basis of the structure determined for (1e) the process idealised as (2) $\rightleftharpoons$ (3) is implicated. Because of the phosphite substitution, rapid inversion of S(1), S(2), and S(3) can only ever make S(1) and S(3) time-averaged equivalent and this pair will always be distinct from S(2), which is effectively *trans* to the $P(OMe)_3$. By reference to the (2) $\rightleftharpoons$ (3) process, it can be seen that rapid inversion of S(2) effects averaging of S(1) and S(3) independent of whether inversion at these atoms occurs rapidly or not. In fact, the i.r. spectra of (1e)—(1h) at room temperature all show evidence for the existence of two isomers, and thus of inversion at S(1) and S(3).

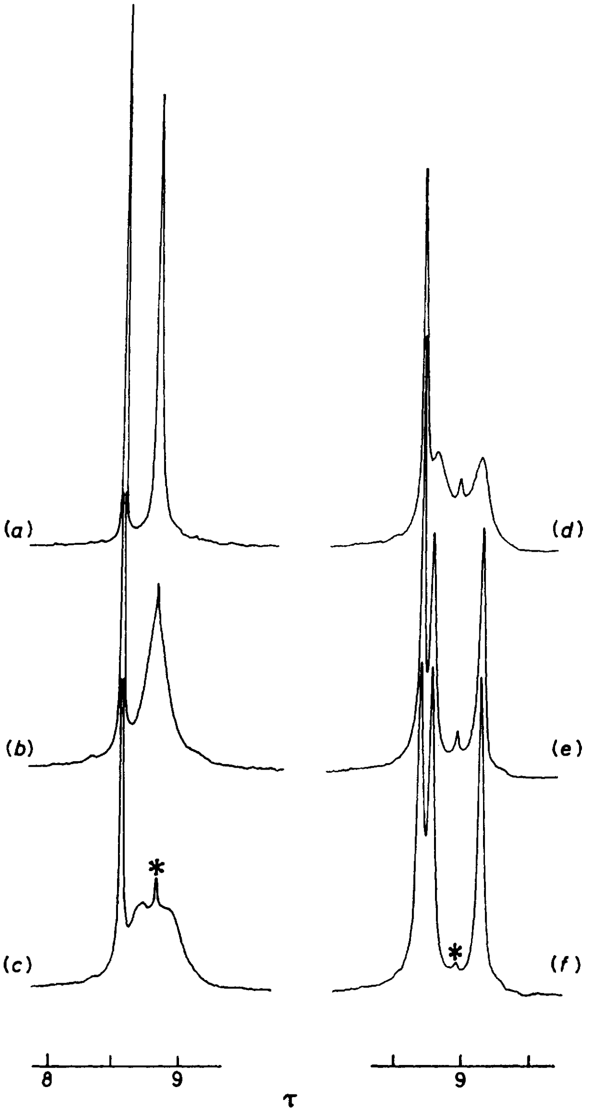

FIGURE 8 Proton n.m.r. spectrum of (1e) at various temperatures in $CDCl_3$: 62 (*a*); 22 (*b*); 12 (*c*); 2 (*d*); −18 (*e*); and −53 °C (*f*). Impurity denoted by asterisk

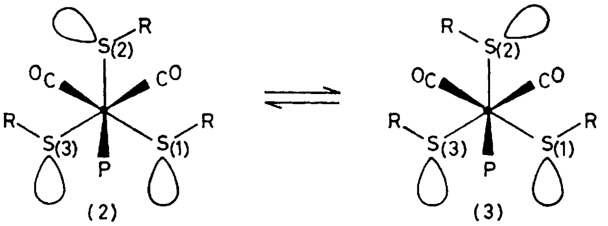

(2) (3)

Inversion at S(2) is the rate-controlling factor in the averaging process and is, not unexpectedly, affected by the nature of the *trans* phosphorus ligand. Free energies of activation for the averaging, and therefore of inversion at S(2), are readily derived [20] from the n.m.r. coalescence temperatures and are collected in Table 7. It can be seen that the highest barrier obtains when the least effective σ donor, $P(OMe)_3$, is *trans* to S(2), and that the barrier is lower for the phosphines $PMePh_2$, PMe_2Ph, and PMe_3. However, for each of the latter the barrier is effectively identical, so inversion at S(2) is clearly not influenced by relatively minor modifications in the nature of the *trans* ligand. These very low barriers for sulphur inversion may in part be attributed to the more basic phosphines increasing electron density in the *trans* Mo–S bond and causing the Mo–S–C angle to expand and therefore more nearly approach the transitional trigonal angle. The barrier to sulphur inversion in $[\{Ru(CO)(\mu\text{-}SCH_2Ph)(\eta\text{-}C_5H_5)\}_2]$ [2] was found to be *ca.* 59 kJ mol^{-1}, close to those derived for the dimolybdenum complexes. Barriers to sulphur inversion in mononuclear transition-metal complexes are generally higher (55—70 kJ mol^{-1}), although still lower than those found in sulphoxides and sulphonium ions (100—150 kJ mol^{-1}).[21] It has been suggested that co-ordination with a transition metal reduces inversion barriers by stabilising the transitional trigonal configuration of sulphur through ($p\rightarrow d$)-π-orbital overlap.[22] There seems no reason why metal→sulphur ($d\rightarrow d$)π or ($p\rightarrow d$)π should not also lower the energy of the transition state. In any event, it might be expected that inversion of sulphur bonded to two transition metals would experience a still lower barrier than that achieved by one. The barriers derived here appear to bear this out, despite the possible counteraction of ring-strain effects. However, the recent

TABLE 7

Activation energies for inversion of sulphur

Complex	T_c/K	$\Delta\nu$/Hz	$\Delta G^{\ddagger}$/kJ mol^{-1}
(1e)	285	44	58.8
(1f)	223	22	46.9
(1g)	225	18	47.7
(1h)	229	47	46.7

determination of a barrier as low as 28 kJ mol^{-1} for inversion of sulphur co-ordinated to tungsten in $[W(CO)_5\{S(Me)CH(Me)(Ph)\}]$ [23] indicates that caution must yet be exercised in attempting to account for low-energy sulphur inversion in transition-metal compounds.

EXPERIMENTAL

(*a*) *Synthetic and Spectroscopic Studies.*—Infrared spectra were recorded using a Perkin–Elmer 257 spectrometer and calibrated using the absorption of polystyrene at 1 601 cm^{-1}. Hydrogen-1 n.m.r. spectra were obtained with Varian Associates HA100 and JEOL PS 100, and ^{13}C n.m.r. spectra with JEOL PFT 100 instruments. An AEI MS 902 instrument was used for recording mass spectra. Reactions were performed in a nitrogen atmosphere with solvents dried by distillation over calcium hydride (hydrocarbons) or P_4O_{10} (dichloromethane). Microanalyses were carried out in the microanalytical laboratory of the School of Chemistry, University of Bristol. The literature method was used in the preparation of $[MoI(CO)_2(\eta\text{-}C_7H_7)]$.[24] Spectroscopic data for new compounds are collected in Table 1, with physical and analytical data in Table 2.

Preparation of complexes $[Mo_2(CO)_3(\mu\text{-}SR)_3(\eta\text{-}C_7H_7)]$. (*i*) $[Mo_2(CO)_3(\mu\text{-}SMe)_3(\eta\text{-}C_7H_7)]$ (1a). Small quantities of methanethiol were introduced periodically *via* a cold (−78 °C) finger to a mixture of $[MoI(CO)_2(\eta\text{-}C_7H_7)]$ (1.0 g, 2.7 mmol) and NEt_3 (0.41 g, 4.1 mmol) in dichloromethane (50 cm^3) at 0 °C. The mixture was stirred for 2 h, after which time the colour changed from green to dark red and all the iodide appeared (i.r.) to have been consumed. Solvent was then removed under reduced pressure and the dark red residue introduced to a silica gel column (50 × 2 cm). Elution with dichloromethane–hexane (3 : 7) developed an orange band which provided 0.165 g (30%) of brown-black (1a) after recrystallisation from the same solvent, and a green band containing a trace of unreacted $[MoI(CO)_2(\eta\text{-}C_7H_7)]$.

(*ii*) $[Mo_2(CO)_3(\mu\text{-}SEt)_3(\eta\text{-}C_7H_7)]$ (1b). A mixture of $[MoI(CO)_2(\eta\text{-}C_7H_7)]$ (1.0 g, 2.7 mmol), EtSH (0.25 g, 4.1 mmol), and NEt_3 (0.41 g, 4.1 mmol) in dichloromethane (50 cm^3) was stirred for 24 h at room temperature. Chromatography with dichloromethane–hexane (3 : 2) as in (*i*) provided small amounts of $[Mo(CO)_6]$ and $[MoI(CO)_2(\eta\text{-}C_7H_7)]$, with a dark orange band which gave 0.36 g (48%) of black *crystals* (1b).

(*iii*) $[Mo_2(CO)_3(\mu\text{-}SPr^i)_3(\eta\text{-}C_7H_7)]$ (1c). A mixture of $[MoI(CO)_2(\eta\text{-}C_7H_7)]$ (1.0 g, 2.7 mmol), Pr^iSH (0.31 g, 4.1 mmol), and NEt_3 (0.41 g, 4.1 mmol) in dichloromethane (50 cm^3) was stirred for 40 h at room temperature. Chromatography as in (*i*) gave with dichloromethane–hexane (1 : 9) 15 mg of dark brown *crystals* identified tentatively as $[Mo_2(CO)_4(\mu\text{-}SPr^i)_3(\eta\text{-}C_7H_7)_2]$ on the basis of i.r. [ν(CO): 1 999s, 1 987s, 1 948s, and 1 854s cm^{-1} (hexane)] and mass spectra and elemental analyses (Found: C, 46.1; H, 5.5; S, 13.4%; *M*, 711. $C_{27}H_{35}Mo_2O_4S_3$ requires C, 45.6; H, 4.9; S, 13.1%; *M*, 711). Elution with dichloromethane–hexane (1 : 4) gave a dark red band which yielded 0.35 g (44%) of black *crystals* (1c).

(*iv*) $[Mo_2(CO)_3(\mu\text{-}SBu^t)_3(\eta\text{-}C_7H_7)]$ (1d).—A mixture of $[MoI(CO)_2(\eta\text{-}C_7H_7)]$ (1.0 g, 2.7 mmol), Bu^tSH (0.37 g, 4.1 mmol), and NEt_3 (0.41 g, 4.1 mmol) in dichloromethane (50 cm^3) was stirred for 48 h at room temperature. Chromatography as in (*i*) gave some $[Mo(CO)_6]$ and $[MoI(CO)_2(\eta\text{-}C_7H_7)]$, and with dichloromethane–hexane (2 : 5) a dark red band which provided 0.43 g (51%) of black *crystals* (1d).

Preparation of complexes $[Mo_2(CO)_2(PR_3')(\mu\text{-}SBu^t)_3(\eta\text{-}C_7H_7)]$. (*i*) $[Mo_2(CO)_2\{P(OMe)_3\}(\mu\text{-}SBu^t)_3(\eta\text{-}C_7H_7)]$ (1e). Trimethyl phosphite (39 mg, 0.32 mmol) and (1d) (0.2 g, 0.32 mmol) were heated in hexane (75 cm^3) under reflux for 2 h. The reaction mixture was then evaporated to dryness and the residue introduced to an alumina column (20 × 2 cm). Elution with dichloromethane–hexane (1 : 6) removed unreacted (1d), while dichloromethane–hexane (3 : 7) developed a dark orange band which gave 0.1 g (44%) of black *crystals* (1e) following crystallisation from hexane.

(*ii*) $[Mo_2(CO)_2(PMePh_2)(\mu\text{-}SBu^t)_3(\eta\text{-}C_7H_7)]$ (1f). As in (*i*), methyldiphenylphosphine (47 mg, 0.23 mmol) and (1d) (0.15 g, 0.23 mmol), after heating in hexane (75 cm^3) for 1.5 h, gave 92 mg (48%) of black *crystals* (1f).

(*iii*) $[Mo_2(CO)_2(PMe_2Ph)(\mu\text{-}SBu^t)_3(\eta\text{-}C_7H_7)]$ (1g). As in (*i*), dimethylphenylphosphine (33 mg, 0.23 mmol) and (1d) (0.15 g, 0.23 mmol), after heating in hexane (75 cm^3) for 1 h, gave 95 mg (41%) of black *crystals* (1g).

(*iv*) $[Mo_2(CO)_2(PMe_3)(\mu\text{-}SBu^t)_3(\eta\text{-}C_7H_7)]$ (1h). Trimethylphosphine (24 mg, 0.32 mmol) and (1d) (0.2 g, 0.32 mmol) in light petroleum (b.p. 60—80 °C) (75 cm^3) were heated at 80 °C in an evacuated Pyrex tube for 5.5 h. In addition to $[Mo(CO)_6]$, chromatography as in (*i*) gave with dichloromethane–hexane (2 : 3) a dark brown band which provided 76 mg (35%) of brown-black *crystals* (1h).

(*b*) X-*Ray Data Collection and Structure Determination.*—Crystals of $[Mo_2(CO)_2\{P(OMe)_3\}(\mu\text{-}SBu^t)_3(\eta\text{-}C_7H_7)]$ (1e), prepared as above, form as small black parallelepipeds. A single, well formed example, *ca.* 0.2 × 0.2 × 0.15 mm, was selected for analysis and glued to the tip of a quartz fibre with an epoxy-resin adhesive. Preliminary unit-cell and space-group data were obtained from oscillation and zero- and first-layer (equi-inclination) Weissenberg photographs (Cu-K_α *X*-radiation).

Accurate setting and diffraction data were obtained on an Enraf–Nonius CAD 4 four-circle autodiffractometer using graphite-monochromated Mo-K_α radiation ($\lambda_{\alpha 1}$ 0.709 26, $\lambda_{\alpha 2}$ 0.713 54 Å). An initial orientation matrix was calculated following the location of 22 random reflections by the Enraf–Nonius program SEARCH. Fifteen selected reflections ($12 < 2\theta < 26°$) were then accurately centred (program SETANG) and refined by least squares to yield the cell parameters, their associated errors, and the orientation matrix for data collection.

The θ—2θ scan technique was used to record the intensities of one quadrisphere of data ($\pm h + k + l$) within the range $3.0 \leqslant 2\theta \leqslant 50.0°$. Scan widths (SW) were calculated from the equation $SW = A + B\tan\theta$, in which *A* and *B* took values of 0.8 and 0.2 respectively. The intensities of two standard reflections ($3\,\bar{1}\,5$ and $1\,2\,\bar{5}$) were remonitored once every 100 reflections but subsequent analysis of their net counts as individual functions of time revealed no significant decomposition or movement, or source variation, over the course of data collection. After averaging the intensities of equivalent $h\,k\,0$ and $\bar{h}\,k\,0$ reflections the data set was reduced to 5 525 independent non-zero observations.

Crystal data. $C_{24}H_{43}Mo_2O_5PS_3$, $M = 730.6$, Monoclinic, $a = 10.186(7)$, $b = 15.677(7)$, $c = 19.821(15)$ Å, $\beta = 96.31(5)°$, $U = 3\,145.8(17)$ Å^3, D_m not measured, $Z = 4$, $D_c = 1.542$, $F(000) = 1\,496$, $\mu(Mo\text{-}K_\alpha) = 10.5$ cm^{-1}, space group $P2_1/n$ (alternative setting of $P2_1/c$, C_{2h}^5, no. 14) from systematic absences.

Data were corrected for Lorentz and polarisation effects (but not for *X*-ray absorption) and the molybdenum atoms located from analysis of a three-dimensional Patterson synthesis. After three cycles of full-matrix least-squares refinement of the metal positional and isotropic thermal parameters an electron-density difference synthesis revealed all remaining non-hydrogen atoms.

On the basis of an examination of the variations of av.(Δ^2F) with F_o and sinθ, F_o moduli were subsequently weighted according to $w^{-1} = \sigma^2(F_o) + 0.03F_o - 3.0 \sin\theta$. All atoms were allowed anisotropic thermal motion and the 317 resulting variables (including *F* scale and overall temperature factors) were divided between three roughly equally dimensional blocks. In the final stages, reflections were included in structure-factor calculations only if $I \geqslant 2.0\sigma(I)$ (3 760 data) or $2.5\sigma(I) > I$ and $|F_c| \geqslant F_o$ (1 389 data), this procedure giving a data: variable ratio better than 16 : 1.

Refinement continued until no significant change occurred in any variable: *R* 0.046, *R'* 0.054. A final difference Fourier (0.4 Å resolution, all data) was featureless apart from the relatively high noise usually associated with the choice of a low $I/\sigma(I)$ criterion, and could not furnish hydrogen-atom positions. Furthermore, use of a standard sharpening technique [summing to a maximum $(\sin\theta)/\lambda$ of 0.5] gave results that were, at best, uncertain and hydrogen atoms accordingly remain absent.

The scattering factors of refs. 25 (Mo) and 26 (S, P, O, and C) were taken with appropriate correction for both components of anomalous dispersion.[27] Table 6 lists the derived atomic co-ordinates. Thermal parameters and a comparison of $|F_o|$ *vs.* F_c are deposited as Appendices * A and B respectively. All calculations were performed with the '*X*-RAY '72'[28] crystallographic system implemented on the CDC 7600 machine at the University of London Computer Centre. Figures were constructed using Johnson's ORTEP.

We are grateful to the S.R.C. for the award of Research Studentships (to I. B. B. and P. J. N.) and to Dr. M. B. Hursthouse (Q.M.C., London) for diffractometer facilities.

[1/343 *Received, 27th February,* 1981]

---

* All Appendices are contained within Supplementary Publication No. SUP 23114 (25 pp.). For details see Notices to Authors, No. 7, *J. Chem. Soc., Dalton Trans.*, 1980, Index issue.

REFERENCES

[1] Part 6, S. C. Carleton, F. G. Kennedy, and S. A. R. Knox, preceding paper.

[2] S. D. Killops and S. A. R. Knox, *J. Chem. Soc., Dalton Trans.*, 1978, 1260.

[3] D. Mohr, H. Wienand, and M. L. Ziegler, *Z. Naturforsch., Teil B*, 1976, **31**, 66.

[4] D. Mohr, H. Wienand, and M. L. Ziegler, *J. Organomet. Chem.*, 1977, **134**, 281.

[5] I. B. Benson, S. A. R. Knox, P. J. Naish, and A. J. Welch, *J. Chem. Soc., Chem. Commun.*, 1978, 878.

[6] A. J. Welch, *Inorg. Chim. Acta*, 1977, **24**, 97.

[7] R. Bowerbank, M. Green, H. P. Kirsch, A. Mortreux, L. E. Smart, and F. G. A. Stone, *J. Chem. Soc., Chem. Commun.*, 1977, 245.

[8] N. W. Alcock, *Acta Crystallogr., Sect. B*, 1977, **33**, 2943.

[9] M. Mathew and G. J. Palenik, *J. Organomet. Chem.*, 1973, **61**, 301.

[10] D. L. Stevenson and L. F. Dahl, *J. Am. Chem. Soc.*, 1967, **89**, 3721.

[11] N. G. Connelly and L. F. Dahl, *J. Am. Chem. Soc.*, 1970, **92**, 7470.

[12] P. J. Vergamini, H. Vahrenkamp, and L. F. Dahl, *J. Am. Chem. Soc.*, 1971, **93**, 6327.

[13] L. Ricard, J. Estienne, and R. Weiss, *Inorg. Chem.*, 1973, **12**, 2182.

[14] M. Elian, M. M. L. Chen, D. M. P. Mingos, and R. Hoffmann, *Inorg. Chem.*, 1976, **15**, 1148.

[15] M. Green, H. P. Kirsch, F. G. A. Stone, and A. J. Welch, *Inorg. Chim. Acta*, 1978, **29**, 101.

[16] A. D. U. Hardy and G. Sim, *J. Chem. Soc., Dalton Trans.*, 1972, 1900.

[17] R. M. Kirchner and J. A. Ibers, *Inorg. Chem.*, 1974, **13**, 1667.

[18] M. G. B. Drew and J. D. Wilkins, *J. Chem. Soc., Dalton Trans.*, 1975, 1984.

[19] M. G. B. Drew, *J. Chem. Soc., Dalton Trans.*, 1972, 1329.

[20] D. Kost, E. H. Coulson, and M. Raban, *Chem. Commun.*, 1971, 656.

[21] J. B. Lambert, *Top. Stereochem.*, 1971, **6**, 19.

[22] E. W. Abel, G. W. Farrow, K. G. Orrell, and V. Šik, *J. Chem. Soc., Dalton Trans.*, 1977, 42.

[23] J. H. Eekhof, H. Hogeveen, R. M. Kellogg, and E. Klei, *J. Organomet. Chem.*, 1978, **161**, 183.

[24] 'Organometallic Syntheses,' eds. J. J. Eisch and R. B. King, Academic Press, New York, 1965, vol. 1.

[25] D. T. Cromer and J. T. Waber, *Acta Crystallogr.*, 1965, **18**, 104.

[26] D. T. Cromer and J. B. Mann, *Acta Crystallogr., Sect. A*, 1968, **24**, 321.

[27] 'International Tables for *X*-Ray Crystallography,' Kynoch Press, Birmingham, 1974, vol. 4.

[28] Technical Report TR192 of the Computer Science Center, University of Maryland, June 1972.